Structural Change and Properties of Pseudobinary Nitrides Containing AlN†

Yukio MAKINO* **and Shoji MIYAKE** **

Abstract

Structural change in pseudobinary nitrides containing AlN was predicted by using the structural map of AB compounds. According to the prediction, CrN shows the highest maximum solubility of AlN for transition metal nitrides with B1 structures. The predicted maximum solubility for CrN and TiN showed excellent agreement with those experimental results. It was indicated that the properties of pseudobinary nitrides such as hardness and anti-oxidation were improved with increasing AlN content, unless these nitrides changed from B1 structure to B4.

KEY WORDS: (Pseudobinary Nitride), (Structural Map), (Band Parameter), (Structural Change), (Hardness)

1. Introduction

Various superhard materials such as carbon nitride and nano-composites have been widely synthesized by various PVD processing[1)-3)]. Carbon nitride was predicted by Cohen, based on simple semi-empirical and pseudopotential approaches[4),5)]. The important parameter in the prediction of superhard carbon nitride is the interatomic distance and its hardness higher than diamond was predicted by the calculation of the bulk modulus based on the relation between the covalent band gap and the interatomic distance[6)]. In other words, the high hardness of carbon nitride is based on the estimation of bond strength. On the other hand, several models of the origin of high hardness for the nano-composite materials have been proposed[7),8)].

Nitrides are the important component for obtaining high hardness, as shown in researches on the superhard materials. From the middle of the last century, nitrides and their composites have been widely investigated for the use as hard and anti-oxidation materials[9),10)]. Among these materials, titanium nitride is one of the most popular nitrides and a vast number of reports on TiN and its composites have been presented[11)-13)]. In the results on the binary nitride consisting of TiN and AlN, it has been indicated that the addition of aluminum nitride (AlN) is quite effective for anti-oxidation property as long as these nitrides are in the form of a single phase with B1(NaCl) structure. However, large amounts of AlN causes the decomposition of B1 single phase, resulting in the formation of a mixed phase of B1 and B4(wurtzite) structures. Because change of the B1 single phase to a mixed phase degrades its anti-oxidation property, it is important for anti-oxidation property of the Ti-Al-N ternary coating to decide the solubility limit of AlN for TiN. Further, the solubility limit of AlN for another transition metal nitride is also important when a new nitride with a high anti-oxidation property is required.

In this study, the maximum solubility of AlN for transition metal nitrides with B1 structure was estimated by a semi-empirical approach based on the band parameters. These maximum solubilities were verified by comparing with the previous results and the dependency of hardness and anti-oxidation property on the structural change of pseudobinary nitride was discussed.

2. Structural map and prediction of maximum solubility of AlN into transition metal nitride

† Received on Feb. 1, 2002

* Associate Professor

** Professor

Transactions of JWRI is published by Joining and Welding Research Institute of Osaka University, Ibaraki, Osaka 567-0047, Japan.

In the previous paper, it has been reported that AB-type compounds with various crystal structures can be separately placed in the two dimensional structural map based on the band parameters[14], which are named as hybrid function(H) and band gap parameter (S) and constructed on the basis of the bond orbital model[15] and pseudopotetial radius[16]. Physical meanings of the band parameters can briefly be explained by the schematic energy diagram based on the bond orbital model. According to the bond orbital model, the band gap(E_g) can be expressed by the electronic energies of valence electrons and hybrid covalent energy. For the zincblende structure, the band gap for the Γ point at the center of the Brillouin zone can be expressed as follows[17];

$$\begin{aligned} E_g &= -[\{\varepsilon_p(c)-\varepsilon_s(c)\}+\{\varepsilon_p(a)-\varepsilon_s(a)\}]/2 \\ &+[\{\varepsilon_s(c)-\varepsilon_s(a)\}^2/4+\{4E_{ss}\}^2]^{1/2} \\ &+[\{\varepsilon_p(c)-\varepsilon_p(a)\}^2/4+\{4E_{xx}\}^2]^{1/2} \end{aligned} \quad (1)$$

where $\varepsilon_s(c)$, $\varepsilon_s(a)$, $\varepsilon_p(c)$ and $\varepsilon_p(a)$ are the electronic energies of the s and p electrons of cationic and anionic atoms, and E_{ss} and E_{xx} are the covalent terms which are expressed by $V_{ss\sigma}$ and $(V_{pp\sigma}/3+2V_{pp\pi}/3)$. $V_{ss\sigma}$, $V_{pp\sigma}$ and $V_{pp\pi}$ are the off-diagonal matrix elements for ssσ, ppσ and ppπ bondings, respectively. The first term in equation (1) corresponds to a band gap reduction parameter due to the formation of a crystalline state. The second and third terms in equation (1) correspond to the contributions of s and p electrons to the energy difference between bonding and anti-bonding levels. Here, we approximate the sum of second and third terms in the equation (1) by following forms[18];

$$\begin{aligned} &[\{\varepsilon_s(c)-\varepsilon_s(a)\}^2/4+(4E_{ss})^2]^{1/2} \\ &+[\{\varepsilon_p(c)-\varepsilon_p(a)\}^2/4+(4E_{xx})^2]^{1/2} \\ &\cong (\alpha_s/n_{av})^{1/2}+(\alpha_p/n_{av})^{1/2} \\ &\equiv H_{sp}(=H: \textit{in general case}) \end{aligned} \quad (2)$$

where $\alpha_s=|(Z/r_s)^{1/2}{}_A-(Z/r_s)^{1/2}{}_B|$ and $\alpha_p=|(Z/r_p)^{1/2}{}_A-(Z/r_p)^{1/2}{}_B|$, and $(Z/r_s)^{1/2}$ and $(Z/r_p)^{1/2}$ are the orbital electronegativities of s and p electrons, respectively. Further, r_s, r_p and Z are the Zunger's pseudopotential radii of s and p electrons and valence charge for each constituent atom. Secondly, the first term (the gap reduction term) of the equation (1) was assumed by the following expression;

$$\begin{aligned} &[\{\varepsilon_p(c)-\varepsilon_s(c)\}+\{\varepsilon_p(a)-\varepsilon_s(a)\}]/2 \\ &\cong [\{S_{sp}(A)+S_{sp}(B)\}/n_{av}]^{1/2} \\ &\equiv S_{sp}(=S: \textit{in general case}) \end{aligned} \quad (3)$$

where $S_{sp}(M)=|(Z/r_s)^{1/2}{}_M-(Z/r_p)^{1/2}{}_M|$(M;A or B). Both H and S are called as the *band parameter* and the former and latter are called the *hybrid function* and *gap reduction parameter*(in this case for sp bonding). **Figure 1** shows a schematic energy diagram for the above-described approximation[19]. When d electrons affect the band gap reduction for sp-bonded compounds, we estimate the gap reduction parameter by using S_{sd} in the equation (3) instead of S_{sp}, where $S_{sd}(M)=|(Z/r_s)^{1/2}{}_M-(Z/r_d)^{1/2}{}_M|$ and r_d is Zunger's pseudopotential radius of d electron. Details of the two band parameters are described elsewhere.

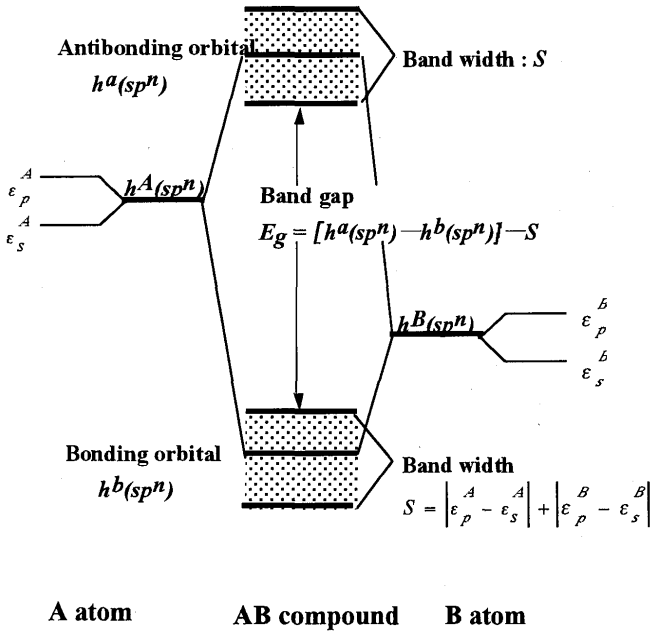

Fig.1 Schematic energy diagram for the sp-bonded compound based on the bond orbital model. (ε^s_A, ε^p_A etc. are the energies of s and p electrons of A and B atoms. $h^A(sp^n)$ and $h^B(sp^n)$ are the hybrid orbitals. n is 3 for a typical case of spn bonding. The general case for sp^n bonding is illustrated here.

When the plot for InN is replotted by changing its bonding mode from spd-type to sp-type in the structural map for 333 AB compounds, we can illustrate a partial structural map with straight boundary lines and constant H/S ratios. **Figure 2** shows the partial structure map extracted from the structural map for 333 AB compounds[14]. Almost all nitrides, carbides and some oxides, except for lanthanide nitrides, are placed in the B1 domain of Fig.1. Using the boundary line between B1 and B4 domains in the partial structure map, we can predict the maximum solubility of B4 nitrides into transition metal nitrides by the following equations;

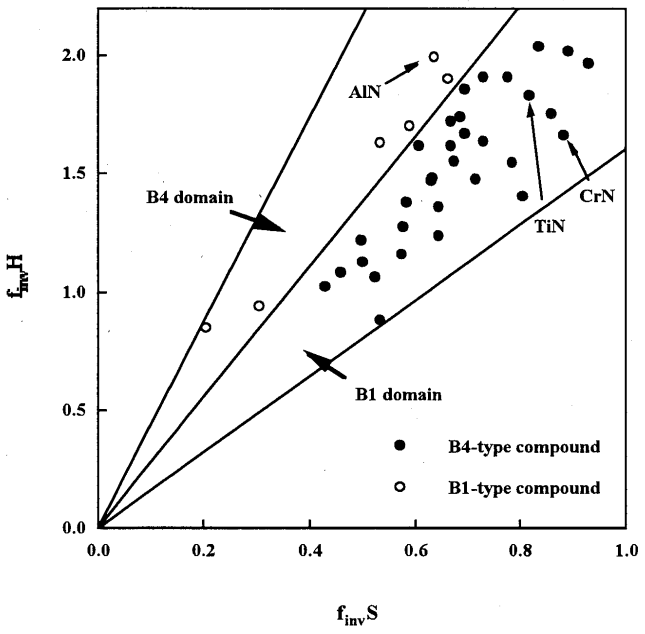

Fig.2 Partial structural map for B1 and B4 compounds constructed by two band parameters[14].

$$x = \frac{f_{inv(MN)}(2.78S_{MN} - H_{MN})}{f_{inv(AlN)}(H_{AlN} - 2.78S_{AlN}) - f_{inv(MN)}(H_{MN} - S_{MN})} \quad (4)$$

where H_{MN}, S_{MN} and $f_{inv(MN)}$ are the hybrid function, gap reduction parameter and compositional factor of transition metal nitride(MN), H_{AlN}, S_{AlN} and $f_{inv(AlN)}$ are those of AlN, respectively. The numerical value of 2.78 is the slope of the boundary line between B1 and B4 domains. The numerical values of maximum solubilities of AlN into several transition nitrides with B1 structure are given in **Table 1**[14]. Among the various B1 TM nitrides, it is predicted that the largest maximum solubility of B4 nitride is obtained for CrN. Further, the maximum solubilities correspond to the critical contents at which the crystal structures of these pseudobinary nitrides change from B1 type to B4 type. Considering the oxide form of constituents in the pseudobinary film after oxidation, the film of Cr-Al-N system is predicted to be one of the most suitable pseudobinary nitride for anti-oxidation property, because both Cr_2O_3 and Al_2O_3 are the most effective barriers for oxidation. Thus, the structure map enables us to predict the maximum solubilities of B4 nitrides into B1 transition metal nitrides, in other words, the critical composition for the phase change from B1-type structure to B4-type one in the pseudobinary nitrides.

3. Structural change and the hardness of pseudo-binary nitride containing AlN

Among various films of pseudobinary nitrides between transition metal nitride and AlN, Ti-Al-N system have been most widely investigated by various PVD and CVD methods. Accordingly, we focus first on the structural change and hardness of the Ti-Al-N films, and secondly on these problems of the Cr-Al-N system, because the system is predicted to be the best candidate from the standpoint of maximum solubility of AlN.

Ti-Al-N pseudobinary films have been extensively investigated by various deposition methods[20)-22)]. In **figure 3**, typical results on the structural change of Ti-Al-N pseudobinary films are shown by using the relation between lattice constant and AlN content in the film[23)-25)]. The predicted maximum solubility of AlN in TiN shows a good agreement with the experimental results. However, Ti-Al-N films with two phases were formed at a lower content of AlN than the maximum solubility for Ti-Al-N system when the optimum conditions for deposition could not satisfied, depending on the deposition method,. For example, substrate temperature has an important effect on the stability of deposited films, as discussed later.

Subsequently, the similar results on the Cr-Al-N films synthesized by magnetron sputtering and pulse laser deposition methods[26)-27)] are shown in the relation between lattice constant and AlN content in the film, as given in **figure 4**. Except for the formation of very small amount of B4 phase at 67mol% AlN content, the prediction for the maxmum solubility of AlN to CrN also

Table 1 The maximum solubilities of B4-type nitrides into B1-type transition metal nitrides predicted by the partial structure map and two band parameters.

	TiN	VN	CrN	ZrN	NbN	HfN	WN
AlN	**65.3%**	72.4%	**77.2%**	33.4%	52.9%	21.2%	53.9%
GaN	87.6	90.8	92.7	65.4	80.8	50.2	81.5
InN	74.3	81.2	83.9	43.6	63.3	29.2	64.3

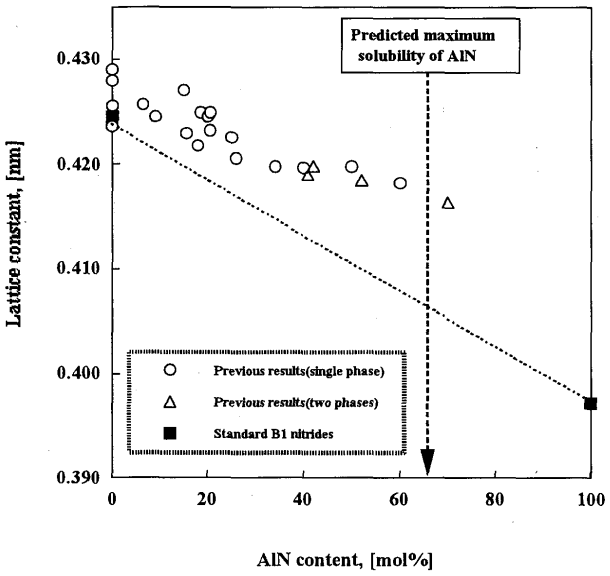

Fig.3 Dependence of lattice constant of pseudobinary Ti-Al-N films synthsized by various PVD methods versus AlN content[23)-25)].

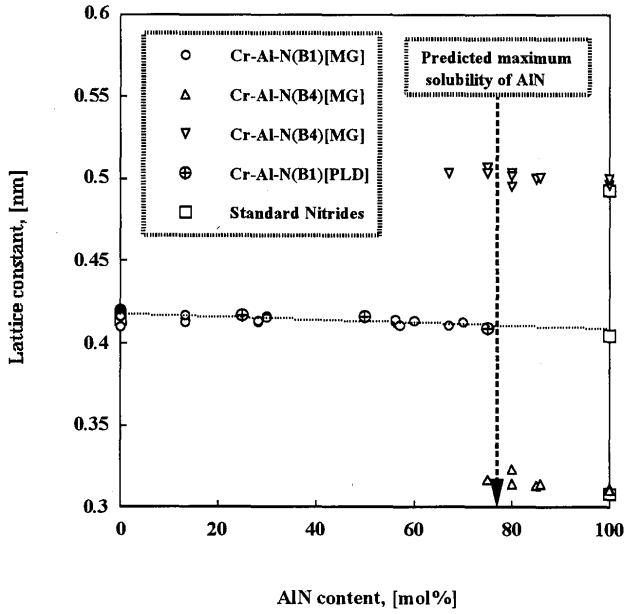

Fig.4 Dependence of lattice constants of B1 and B4 phases in the Cr-Al-N films synthesized by various methods on the AlN content.(MG; magnetron sputtering method, PLD; pulse laser deposition method)

shows excellent agreement with the experimental results. Thus, the prediction based on the structural map and band parameters can be available for the critical content of the phase change from B1 phase to B4 in the pseudobinary TM-Al-N nitrides.

As described above, it has been reported that the properties of TM-Al-N pseudobinary nitride films are strikingly affected by the structural change. In most cases, the properties such as hardness, oxidation behavior and electric resistivity were examined and abrupt changes on these properties were observed. Here, we examine the recent result on hardness of Ti-Al-N synthesized by magnetron sputtering[28)] and Cr-Al-N films synthesized by pulse laser deposition method[29)], comparing with a typical result of Ti-Al-N films by arc ion plating method[23)]. The change of hardness with the AlN content is shown in **Figure 5** by using the scale of relative hardness to the respective hardness of CrN and TiN, respectively. The increase of hardness in the Cr-Al-N films is observed up to an AlN content close to the critical value for the structural change from B1 to B4. On the other hand, the maximum of relative hardness depends on the deposition method. In the Ti-Al-N films synthesized by the IBAD(ion beam assisted deposition) method, the experimental maximum of the hardness shows an excellent agreement with the predicted AlN content. The excellent agreement is also obtained in the Ti-Al-N films synthesized by the arc ion plating method. On the contrary, no good agreement is not obtained in the Ti-Al-N films synthesized by the magnetron sputtering method and the maximum of relative hardness is observed at the content of 50mol% AlN. The reason for this disagreement is clearly explained by the substrate temperature. Because these films were deposited at 723 K, the films begin to change their structure to B4 at contents of AlN in excess of 50 mol%, and a mixed phase of B1 and B4 appears in the contents at 60mol% and 70mol%

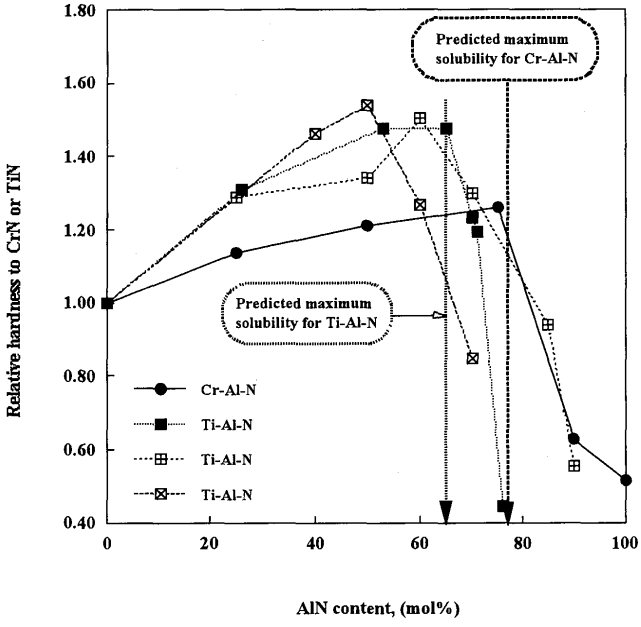

Fig.5 Dependence of relative hardness of Cr-Al-N and Ti-Al-N pseudobinary nitride films to the single phase CrN or TiN on the AlN content.

AlN. Accordingly, the AlN content for the maximum of hardness coincides with the content for the change of the film structure from B1 to B4, though the experimental AlN content disagrees with the predicted value. Comparing with the result on the films deposited at 573K by the same magnetron sputtering method, as shown in Fig.4, the difference of 150K in the substrate temperature causes the shift of the maximum hardness, that is, structural change to the lower content of AlN. The phenomenon can be quite naturally interpreted by the unstableness of the pseudobinary nitride at higher substrate temperature.

Finally, we discuss the anti-oxidation properties of pseudobinary nitrides. Oxidation behavior of Ti-Al-N film has been examined by several investigators[11),12),24)]. Although no systematic result on oxidation of Ti-Al-N film could be found, it is generally accepted that the dissolution of AlN into TiN is quite effective for anti-oxidation property of Ti-Al-N film. For example, the addition of AlN heightens initial temperature for oxidation by more than 200°C[24)]. It was also indicated that the rate constant for oxidation in $Ti_{0.5}Al_{0.5}N$ film could be lowered to a similar order to AlN[11)] and the activation energy for oxidation was heightened by more than twice, compared with TiN[11)]. It is considered that the improvement of oxidation resistance of TiN by AlN is attributable to the stabilization of the 3d electron energy of titanium. However, clear proofs of the improvement of oxidation resistance for pseudobinary nitrides are required.

4. Summary

Structural change from B1 phase to B4 in TM(transition metal)-Al-N pseudobinary nitride was interpreted by the structural map for AB compounds and band parameters. The predicted contents of AlN for TM-Al-N nitrides show the excellent agreement with experimental results. It was indicated that the addition of AlN to transition metal nitride can improve the properties such as hardness and oxidation resistance as long as the B1 structure is maintained.

References

1) A.Y.Liu and M.L.Cohen; Science, 245(1989)841-842.
2) J.Musil and J.Vlcek, Surface and Coatings Technol., 142-144(2001)557-566.
3) S.Veprek; j. Vac. Sci. Technol., 17(1999)2401-2420.
4) M.L.Cohen; Phys. Rev., B32(1985)7988-7991.
5) P.K.Lam, M.L.Cohen and G.Martinez; Phys. Rev., B35(1987)9190-9194.
6) J.C.Phillips; Rev. Mod. Phys., 42(1970)317-356.
7) M.Shinn, L.Hultman and S.A.Barnett; J. Mater. Res., 7(1992)901-911
8) X.Chu and S. A.Barnett; J. Appl. Phys., 77(1995)4403-
9) L.Hultman; Vacuum, 57(2000)1-30.
10) J.Musil, P.Karvánková and J.Kasl; Surface and Coatings Technol., 139(2001)101-109.
11) D.McIntyre, J.E.Greene, G.Hakånsson, J.-E.Sundgren and W.-D.Münz; J. Appl. Phys., 67(1990)1542-53.
12) H.Ichimura and A.Kawana; J. Mater. Res., 8(193)1093-1100.
13) F.Adibi, I.Petrov, L.Hultman, U.Wahlström, T.Shimizu, D.McIntyre and J.E.Greene; J. Appl. Phys., 69(1991) 6437-6450.
14) Y.Makino; ISIJ International, 38(1998)925-934.
15) W.A.Harrison; Electronic Structure and The Properties of Solids, Freeman, San Francisco, CA, (1980) Chap.3.
16) A.Zunger; Phys. Rev., B22(1980)5839-5872.
17) C.D.J.Chadi and M.L.Cohen; Phys. Status Solidi, 68(1975)405-419.
18) Y.Makino; Intermetallics, 2(1994)55-66.
19) Y.Makino; Mater. Sci. Eng., A192/193(1995)77-82.
20) J.Musil and H.Hruby; Thin Solid Films, 365(2000)104-109.
21) M.-S.Wong, G.-Y. Hsiao and S.Y.Yang, Surface and Coatings Technol., 133/134(2000) 160-165.
22) S.Shimada and M.Yoshimatsu; Thin Solid Films, 370(2000)146-150.
23) J.R.Roos, J.P.Celis, E.Vancoille, H.Veltrop, S.Boelens, F.Jungblut, J.Ebberink and H.Homberg; Thin Solid Films, 193/194(1990)547-556.
24) T.Ikeda and H.Satoh; Thin Solid Films, 195(1991)99-110.
25) U.Wahlström, L.Hultman, J.-E.Sundgren, F.Adibi, I.Petrov and J.E.Greene; Thin Solid Films, 235(1993)62-70.
26) A.Sugishima, H.Kajioka and Y.Makino; Surface and Coatings Technol., 97(1997)590-594.
27) Y.Makino and K.Nogi; Surface and Coatings Technol., 98(1998)1008-1012.
28) M.Zhou, Y.Makino, M.Nose and K.Nogi; Thin Solid Films, 339(1999)203-208.
29) M. Hirai, Y. Ueno, T.Suzuki, W. Jiang, C. Grigoriu, and K.Yatsui:, Jpn. J. Appl. Phys. 40(2001) 1056-1060.
30) T.Suzuki, Y.Makino, M.Samandi and S.Miyake; J. Mater. Sci., 35(2000)4194-4199.